Short communication

Investigation on modified natural rubber gel polymer electrolytes for lithium polymer battery

A.M.M. Ali [a,b,∗], R.H.Y. Subban [a,b], H. Bahron [a], M.Z.A. Yahya [c], A.S. Kamisan [c]

[a] Faculty of Applied Sciences, Universiti Teknologi MARA, 40450 Shah Alam, Selangor, Malaysia
[b] Institute of Science, Universiti Teknologi MARA, 40450 Shah Alam, Selangor, Malaysia
[c] Department of Defence Science, Universiti Pertahanan Nasional Malaysia, 57000 Kuala Lumpur, Malaysia

HIGHLIGHTS

► Gel polymer electrolytes-based methyl-grafted natural rubber has been investigated.
► Conductivity temperature dependence of GPE exhibited Vogel−Tamman−Fulcher type.
► The anodic decomposition limit of the GPE stable up to 4.2 V versus Li^+/Li.
► Cycling performance of lithium cell using $LiCoO_2$ cathode stable at room temperature.

ARTICLE INFO

ABSTRACT

Non-aqueous gel polymer electrolytes (GPEs) consisting of 30% poly(methyl methacrylate)-grafted natural rubber (MG30), lithium triflate (LiTf), and ethylene carbonate (EC) dissolved in tetrahydrofuran are examined as electrolytes for lithium polymer batteries. The AC impedance technique is employed at room and elevated temperatures in the frequency range between 0.1 kHz and 1.0 MHz to optimize the conductivity of MG30−LiTf samples. The membrane containing 35 wt.% of LiTf is found to exhibit the highest ionic conductivity. The introduction of EC resulted in increased ionic conductivity of up to 8.95×10^{-3} S cm^{-1} at room temperature for the composition MG30(15):LiTf(9):EC(76). The temperature dependence conductivity for all systems studied is of the Vogel−Tamman−Fulcher type. Attenuated total reflectance-Fourier transformed infrared spectroscopic analysis suggested that EC penetrated between the polymer chains without perturbing the complexation that occurred between the polymer and lithium salt. The Li/Li$^+$ interface stability is established to withstand voltages greater than 4.2 V. A lithium polymer half-cell is successfully fabricated using MG30-based GPE and the cell with configuration of Li/MG30:LiTf:EC/LiCoO$_2$ is found to show good cycling efficiency at room temperature.

© 2013 Elsevier B.V. All rights reserved.

1. Introduction

Solid and/or gel polymer electrolytes (SPEs and/or GPEs) have recently received a great deal of attention because of possible application in various electrochemical devices [1−3]. These electrolytes exhibit a number of advantages, which include providing ionic transport at par with liquid electrolytes, being chemically compatible with electrode materials, possessing good mechanical strength and flexibility, as well as being leak free. However, studies on lithium ion batteries that use liquid electrolytes are reported to encounter problems on the vitality of liquid electrolytes [4]. The improvement of the conductivity of gel polymeric systems is an important aspect of research activities on this field. Attempts have been made to enhance the electrical properties of the SPEs and/or GPEs for use in lithium polymer batteries [5,6].

Among all natural rubber (NR)-based polymer electrolytes, epoxidized NR or poly(methyl methacrylate)-grafted NR (PMMA-g-NR) is known to display superior ionic conductivity. Reports on modified NR as polymer electrolytes showed the highest conductivity for salted NR in the order of 10^{-5} S cm^{-1} and for double-plasticized NR systems up to the order of 10^{-4} S cm^{-1} at ambient temperature [7]. Modified NR also has soft elastomeric characteristics at room temperature, with good elasticity resulting in excellent electrode−electrolyte contact. The introduction of plasticizers will also alter the physical and electrical properties of the electrolytes [8−11]. Reports on modified NR-based polymer

electrolytes have been extensively studied [12–17]. However, these studies did not fabricate any batteries with electrolytes.

In the present work, SPEs based on 30% PMMA-g-NR (MG30) doped with lithium triflate (LiTf) at various stoichiometric compositions were studied to obtain the highest ionic conductivity. The optimized ionic conductivity composition of SPEs has been swelled in organic-solvent ethylene carbonate (EC) to prepare GPEs. The prepared samples were then characterized by attenuated total reflectance-Fourier transformed infrared (ATR-FTIR), differential scanning calorimetry (DSC), AC impedance spectroscopy, lithium transference number, and linear sweep voltammetry. A half-cell was fabricated using commercial cathode lithium cobalt oxide (LiCoO₂).

2. Experimental

MG30 was obtained commercially from the Rubber Research Institute of Malaysia (RRIM), whereas LiTf and EC were supplied by Aldrich. The lithium salt was dried for over 48 h under vacuum at 110 °C, and the plasticizer was distilled over molecular sieve type 4 Å prior to use. All polymer electrolytes were prepared using the solution cast technique.

The SPEs were prepared by dissolving 1.0 g of MG30 with different amounts of lithium salt in 25 ml tetrahydrofuran (THF) solvent and subsequently stirred continuously for several hours. The solutions were then cast into Petri dishes, and the films were allowed to form at room temperature. The resulting films were then kept dry in a vacuum oven at 60 °C for 48 h prior to conductivity testing. The optimized compositions with the highest conductivity film were used to prepare GPEs. The MG30 samples were allowed to swell in THF for approximately 48 h before adding different stoichiometric ratios of LiTf–EC liquid electrolytes. The mixture was then stirred in a closed Scott bottle for another 24 h at ambient temperature, and the cap of the Scott bottle was then half-opened with continuous stirring at 60 °C until a proportion of the solvent evaporated. The viscous liquids were then cast into Petri dishes and continuously dried in a vacuum oven at 60 °C to remove all residual solvents until the gel films have formed.

The resulting GPE films were kept in a glove box for subsequent use. ATR-FTIR spectroscopic studies were conducted using a Perkin–Elmer Spectrum One spectrometer in the frequency range of 650–4000 cm⁻¹. The AC impedance spectroscopy was performed

using a HIOKI 3532-50 LCR Hi Tester in the frequency range of 0.1 kHz–1.0 MHz at a temperature range of 30–110 °C. Linear sweep voltammetry was performed using Auto-Lab Potentiostat/Galvanostat in a cell consisting of a SUS 316 working electrode and lithium metal as counter and reference electrode at a scanning rate of 1.0 mV s⁻¹. The direct current polarization of the cells was conducted by placing the polymer electrolyte films between two lithium metal electrodes in an argon-filled MBRAUN glove box (O₂ < 0.1 ppm; H₂O < 0.1 ppm), and the measurements were taken using the Bruce–Vincent method [18]. A half-cell was fabricated using commercial cathode LiCoO₂.

3. Results and discussion

Fig. 1 shows the FTIR spectra of MG30, LiTf, and EC in plasticized and unplasticized polymer–salt complexes. The peak at 1728 cm⁻¹ in Fig. 1(b) observed in the MG30 sample originated from the C=O band of the ester group in the grafted PMMA side chain. The Li⁺ ← O=C coordination was confirmed by the observed C=O stretching frequency peak located at 1728 cm⁻¹, which has shifted to lower wavenumbers at 1720 cm⁻¹ with reduced relative intensity in the MG30–LiTf samples. The IR peak shifts of triflate ion justify the Li⁺ ← O=C coordination. The CF₃ component was observed at 1224 cm⁻¹ because the ν_s(CF₃) stretching mode has merged with the C–O stretching mode of MG30 at 1272 cm⁻¹ and with the CH₂ twisting mode of MG30 at 1239 cm⁻¹ to form a small shoulder and a broad band centered at 1251 cm⁻¹. The δ_s(CF₃) stretching mode located at 777 cm⁻¹ disappeared in the complexed sample. This phenomenon is possibly attributable to the formation of aggregate ions. Since the δ_s(CF₃) of LiTf is highly sensitive to ionic association, the disappearance of this band is highly indicative of the presence of ionic aggregation of [Li₂TF]⁺ species which has also been observed in other reported work [19]. Such aggregation implies an increase in the number of cluster ions, which could explain why the bulk conductivity is not totally dominated by Li⁺ cations. The ν_s(SO₃) stretching mode at 1044 cm⁻¹ has shifted to 1035 cm⁻¹ with reduced intensity in the MG30–LiTf samples. The shifting of this peak could be related to the number of monodentate ion pairs [20,21] whose presence strongly affects the bulk conductivity of the electrolyte.

LiTf dissociated into ions and formed complexation with the polymer host. However, incorporation of EC did not disturb the
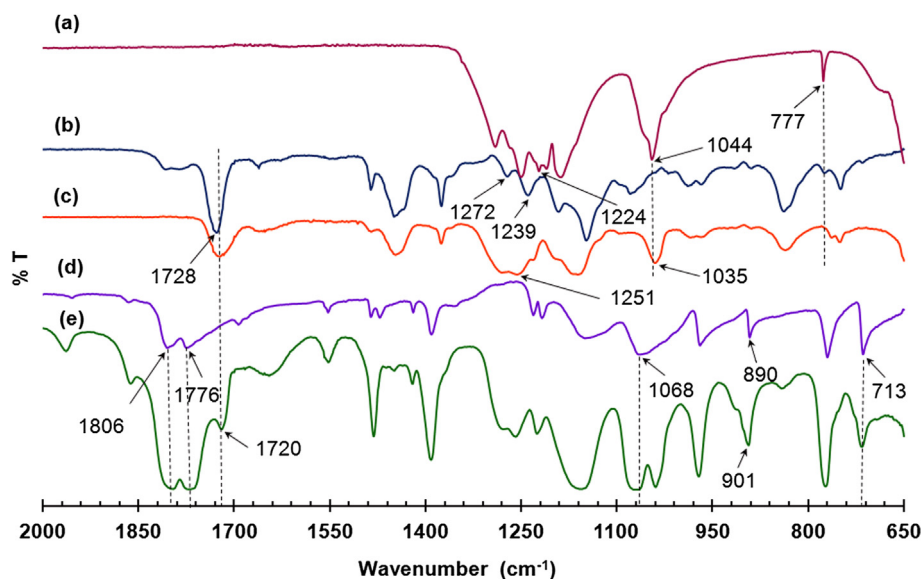

Fig. 1. FTIR spectra of (a) LiTf; (b) MG30; (c) MG30:LiTf (65:35 wt.%); (d) EC and (e) MG30:LiTf:EC (15:9:76 wt.%) at frequency range 650–2000 cm⁻¹.

position of the peaks that appeared in the spectrum of MG30–LiTf. Some new peaks appeared because of the interactions between plasticizer and lithium salt and are manifested in the spectrum of the plasticized samples. The competing interaction between Li^+ and C=O in MG30 and EC can be seen in the spectra shown in Fig. 1(e). The characteristic peaks of EC plasticizer (Fig. 1(d)) at 713 cm^{-1} (C=O bending) and the doublet band (C=O stretching) at 1776 and 1806 cm^{-1} observed in the present study is similar to that reported in the literature [22,23]. The peaks corresponding to C=O doublet stretching mode became broader with little down shift to lower wavenumbers (1771 and 1800 cm^{-1}), while the C=O bending mode is observed to somewhat broaden and remain unshifted with the presence of MG30 and LiTf salt. The EC ring-breathing mode located at 890 cm^{-1} has shifted to 901 cm^{-1} with higher relative intensity and a small shoulder observed at higher wavenumber. The second ring-breathing mode at 1068 cm^{-1} formed a doublet that peaks at 1050 and 1085 cm^{-1}. The position and behavior of these bands signify that EC molecules had permeated into the polymer matrix and established a pseudo-interaction between EC and Li^+. Such interaction is probably due to electrostatic force that exists between the cation and the C=O group of EC as reported by other researchers [24]. In contrary, the peak attributed to $Li^+ \leftarrow$ C=O located at 1720 cm^{-1} in the LiTf–MG30 spectrum is still observed in the EC–MG30–LiTf samples, suggesting that the interaction between Li^+ and C=O of the MG30 is more prominent [25]. Hence, the introduction of plasticizer aided in the dissociation of lithium salt into ions and acted as a lubricant that in turn will enhance the conductivity [8]. Table 1 shows the DSC data of MG30, plasticized and unplasticized MG30 lithium salt complexes. The DSC trace of pure MG30 shows a single T_g at −61.603 °C, signifying that the T_g of MG30 is predominated by NR rather than PMMA ($T_g \approx 90–120$ °C). Upon the addition of LiTf, the T_g was observed to increase, suggesting that the crystalline nature of LiTf contributed to the formation of small crystallites in the samples [26]. T_g appeared to decrease from −70 to −74 °C with the addition of EC plasticizer, showing that the plasticizer disrupted the crystalline phase in the samples [27].

The conductivity data on all films showed a straight line in the Vogel–Tamman–Fulcher (VTF) plot with a regression value between 0.997 and 0.999, indicating that the ionic conductivity mechanism was coupled with the segmental mobility of the polymer [28]. Based on DSC results, no thermal transition occurred in the temperature interval of the measurement. The measurement was conducted above the T_g corresponding to the amorphous rich phase of MG30. The addition of EC in the film proved to have the most significant effect on ionic conductivity, as Fig. 2 illustrates. The increase in conductivity is associated with the effect of plasticizer on the conformational structural arrangement and flexibility of the polymer host. The plasticizer can penetrate into the polymer chains to create more free volume [29,30]. This capability is appropriate for the relatively small molecular size of the plasticizer compared
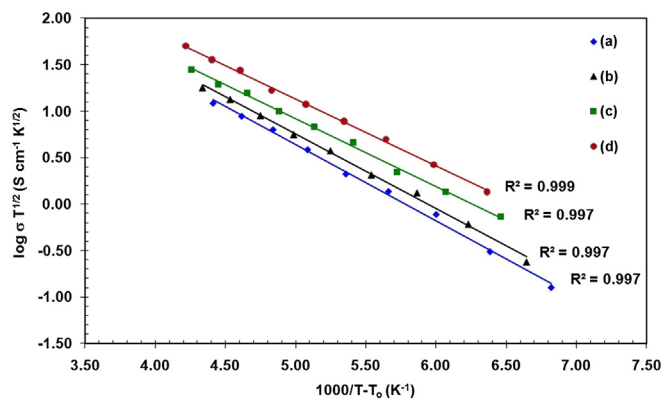
Fig. 2. Temperature dependence of conductivity for the highest conducting composition of MG30:LiTf and MG30:LiTf:EC system with different concentrations (a) 65:35 wt.%; (b) 50:27:23 wt.%; (c) 25:14:61 wt.% and (d) 15:9:76 wt.%.

with the polymer molecules. The effects of penetration deteriorated the attractive forces between polymer–polymer and polymer–salt by inducing a pseudo-interaction between Li^+ and the plasticizer. Such an interaction isolated Li^+ from its surroundings and placed it in between the polymer chain by lowering the coordination force of the ionic environment. This condition resulted in high ionic conductivity at room and elevated temperatures. The activation energy, E_a, was obtained based on VTF plots, as shown in Table 1. The samples with high T_g required more activation energy. The low E_a values of plasticizer enabled the ion to spread through the bulk with less energy.

The lithium transference number, t_{Li^+}, was obtained through a combination of AC and DC techniques [18]. The t_{Li^+} values were observed to increase with increasing plasticizer content (Table 1). A small t_{Li^+} value indicates that the mobility of Li^+ was relatively lower than that of the triflate anions. Fig. 3 shows the linear sweep voltammogram curves of MG30–LiTf based polymer electrolytes. The oxidation peak of MG30:LiTf:EC (15:9:76 wt.%) was observed as stable up to 4.2 V, which is much higher than the oxidation peak of MG30:LiTf (65:35 wt.%) at approximately 1.9 V versus Li/Li^+. This characteristic is influenced by the dynamic formation of Li passivative layer between EC molecules at the Li electrode. Presence of this layer causes the diffusion potential barrier of GPE molecules to keep increasing preventing further decomposition of electrolyte. Initial decomposition of GPE causes formation of this passivative layer that prevents the fresh GPE to be exposed to the Li electrode hence hindering fresh electrolyte from further decomposition.
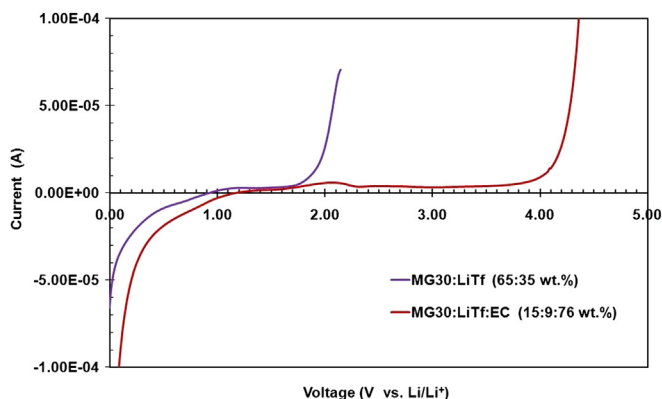
Table 1
Electrical parameters and glass transition temperature values of MG30(65):LiTf(35) based polymer electrolytes containing different wt.% of EC plasticizer.

Electrolytes composition MG30:LiTf:EC (wt.%)	Glass transition temperature, T_g (°C)	Average conductivity $\pm$ standard deviation at 30 °C, $\sigma \times 10^{-3}$ (S cm^{-1})	DC activation energy, E_a (eV)	Lithium transference number, t_{Li^+}
Pure MG30	−61.603	−	−	−
65:35:0	−59.505	0.84 ± 0.10	0.163	0.211
50:27:23	−70.395	1.56 ± 0.31	0.159	0.221
25:14:61	−74.812	4.83 ± 0.25	0.145	0.252
15:9:76	−77.149	8.95 ± 0.18	0.143	0.299

Fig. 3. Linear sweep voltammogram curve of SPE and GPE based on MG30 electrolytes system.

Consequently, the window stability of the GPE film improves. It might be speculated that the presence of EC plasticizer plays an important role at the electrode/electrolyte interface and therefore the plasticized MG30-based polymer electrolytes is suitable for use in lithium polymer batteries using LiCoO$_2$ with a working voltage of 4.2 V [31].

To evaluate the electrochemical performance of MG30-based GPE, lithium polymer cell LiCoO$_2$/MG30 GPE/Li was then fabricated. The assembly of cells was subjected to a preconditioning cycle with a cut-off voltage for charge−discharge of between 4.2 and 3.0 V and a current density of 0.1 mA cm^{-2} before charging the cell to a voltage of 4.2 V. The charge−discharge curves of Li/MG30 GPE/LiCoO$_2$ cell are shown in Fig. 4. The fabricated cell demonstrated a first charge capacity of 97.09 mAh g^{-1} and a discharge capacity of 90.61 mAh g^{-1}, which is a deviation of approximately 39% below the theoretical capacity of LiCoO$_2$ (160 mAh g^{-1}) [32]. This finding is possibly attributable to the fabrication of the cell itself. The LiCoO$_2$ cathode used in the fabricated cell was obtained commercially as factory grade and is typically used in the fabrication of lithium ion batteries using liquid electrolytes. This commercial cathode mixture is composed of 80% LiCoO$_2$, 10% DBP (dibutyl phthalate), 6% super P black, and 4% PVDF (polyvinylidene fluoride) binder coated in aluminum foil. The cell was assembled with MG30 GPE electrolyte sandwiched between LiCoO$_2$ cathode and a lithium metal anode. The thickness of the cathode mixture range from 90 to 120 μm and its mass loading is about 12−14 mg cm^{-2}. The direct lamination between LiCoO$_2$ cathode, GPE, and lithium foil was subjected to capacity fade. During charging, a part of the LiCoO$_2$ cathode was expected to be used to contribute to the specific capacity of the cell. This occurrence was attributable to the physical characteristics of GPE, which made intimate contact at the interface between electrodes and electrolytes without penetrating into the whole cathode mixture, further explaining why the fabricated cell using GPE exhibited a specific capacity lower than the theoretical capacity.

The initial coulombic efficiency (CE) of the cell was approximately 93.33%, with an irreversible capacity of approximately 6.67% in the first cycle. The small drop in the irreversible capacity could possibly be attributable to the formation of a solid electrolyte interphase (SEI) between the lithium anode and the GPE electrolyte. This phenomenon may be attributed to an unavoidable parasitic reaction of EC toward lithium electrode, thereby suggesting that the reaction formed an SEI film comprising LiOH, Li$_2$O and Li$_2$CO$_3$, as reported in the literature [33]. However, the values obtained in the present work are lower than the values observed in
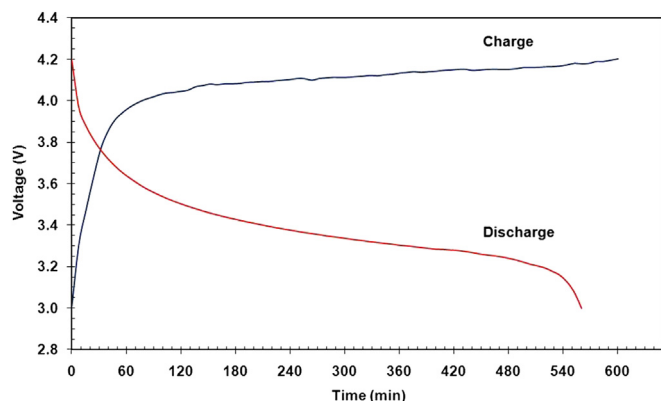

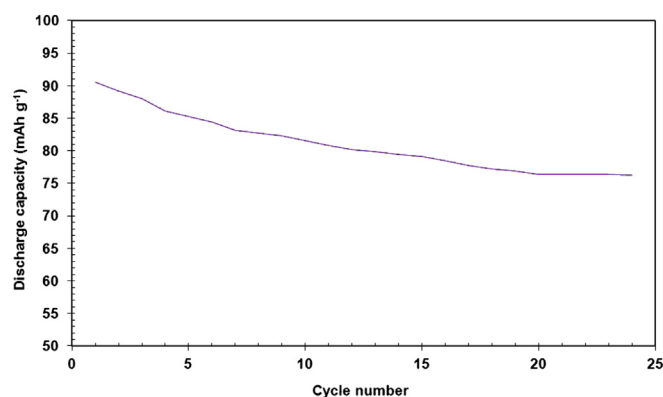**Fig. 5.** Discharge capacities of the Li/MG30:LiTf:EC (15:9:76 wt.%)/LiCoO$_2$ cell as a function of cycle number at 0.1 mA cm^{-2}.

a Li/graphite half-cell using 1 M LiPF$_6$(3):EC/EMC(6) liquid electrolyte with a 13% irreversible capacity in the first cycle [34].

Fig. 5 shows the specific discharge capacities of Li/MG:LiTf:EC (15:9:76 wt.%)/LiCoO$_2$ as a function of cycle number at 0.1 mA cm^{-2}. The cell delivered a discharge capacity of 90.61 mAh g^{-1} at a current density of 0.1 mA cm^{-2}, the value of which slowly decreased upon cycling. After the 10th, 15th, and 20th cycle, the cell delivered discharge capacities of approximately 81.55, 79.15, and 76.38 mAh g^{-1}, respectively. The continuous formations of SEI consume a part of the electrolyte, which corresponds to irreversible capacity fade. However, the discharge capacity is observed to be maintained at 76 mAh g^{-1} after the 20th cycle with CE increasing at approximately 100% throughout cycling. An increase in CE is associated with the reduction of the physical change of GPE electrolytes and interface, which prevented the cell internal resistance from gradually increasing during the charge−discharge cycles. The cell showed a reasonable discharge capacity at a lower C rate (∼0.1 C) however more effort should be done to study the electrolyte performance at higher C-rate and cycle.

4. Conclusion

The effects of EC on MG30−LiTf systems showed excellent suitability as a polymer electrolyte in lithium polymer batteries. The conductivity temperature dependence of the prepared electrolytes was seen to exhibit VTF behavior. The voltammogram of GPE with an anodic decomposition limit of the electrolyte was stable up to 4.2 V versus Li$^+$/Li, making it suitable for possible use in the fabrication of lithium polymer cells using LiCoO$_2$. The cycling performance of the cell using Li anode with MG30:LiTf:EC (15:9:76 wt.%) electrolyte and LiCoO$_2$ cathode at lower C-rate was stable at room temperature.

Fig. 4. First charge−discharge curve for Li/MG30:LiTf:EC (15:9:76 wt.%)/LiCoO$_2$ cell at constant current density 0.1 mA cm^{-2}.

References

[1] H. Gao, Q. Tian, K. Lian, Solid State Ion. 181 (2010) 874−876.
[2] D.K. Pradhan, R.N.P. Choudhary, B.K. Samantoray, Mater. Chem. Phys. 115 (2009) 557−561.
[3] P.C. Barbosa, L.C. Rodrigues, M.M. Silva, M.J. Smith, A.J. Parola, F. Pina, C. Pinheiro, Electrochim. Acta 55 (2010) 1495−1502.
[4] Z. Chen, L.Z. Zhang, R. West, K. Amine, Electrochim. Acta 53 (2008) 3262−3266.

[5] H.M.J.C. Pitawala, M.A.K.L. Dissanayake, V.A. Seneviratne, Solid State Ion. 178 (2007) 885–888.
[6] T. Itoh, Y. Mitsuda, T. Ebina, T. Uni, M. Kubo, J. Power Sources 189 (2009) 531–535.
[7] R. Idris, M.D. Glasse, R.J. Latham, R.G. Linford, W.S. Schlindwein, J. Power Sources 94 (2001) 206–211.
[8] M.Z.A. Yahya, A.K. Arof, Eur. Polym. J. 39 (2003) 897–902.
[9] S. Rajendran, M. Sivakumar, R. Subadewi, Mater. Lett. 58 (2004) 641–649.
[10] A. Ahmad, S.P. Low, F.S.A. Almakhzoom, M.Y.A. Rahman, Adv. Mater. Res. 501 (2012) 44–88.
[11] M.R. Johan, O.H. Shy, S. Ibrahim, S.M. Mohd Yassin, T.Y. Hui, Solid State Ion. 196 (2011) 41–47.
[12] M.D. Glasse, R. Idris, R.J. Latham, R.G. Linford, W.S. Schlindwein, Solid State Ion. 147 (2002) 289–294.
[13] K. Kumutha, Y. Alias, Spectrochim. Acta Part A 64 (2006) 442–447.
[14] F. Latif, M. Aziz, N. Katun, A.M.M. Ali, M.Z.A. Yahya, J. Power Sources 159 (2007) 1401–1404.
[15] A.S. Kamisan, T.I.T. Kudin, A.M.M. Ali, M.Z.A. Yahya, Sains Malays. 40 (2011) 49–54.
[16] K.S. Yap, L.P. Teo, L.N. Sim, S.R. Majid, A.K. Arof, Mater. Res. Innov. 15 (2011) 34–38.
[17] A. Ahmad, M.Y.A. Rahman, M.S. Su'ait, Open Mater. Sci. J. 5 (2011) 170–177.
[18] P.G. Bruce, C.A. Vincent, J. Electroanal. Chem. 225 (1987) 1–17.
[19] S.R. Starkey, R. Frech, Electrochim. Acta 42 (1997) 471–474.
[20] M. Deepa, N. Sharma, S.A. Agnihotry, J. Mater. Sci. 37 (2002) 1759–1765.
[21] D.R. MacFarlane, P. Meakin, A. Bishop, D. McNaughton, J.M. Rosalie, M. Forsyth, Electrochim. Acta 40 (1995) 2333–2337.
[22] C.L. Angell, Trans. Faraday Soc. 52 (1956) 1178–1183.
[23] G. Fini, P. Mirone, B. Fortunata, J. Chem. Soc. Faraday Trans. 69 (1973) 1243–1248.
[24] S. Chintapalli, R. Frech, Solid State Ion. 86–88 (1996) 341–346.
[25] T. Winie, A.K. Arof, Spectrochim. Acta Part A 63 (2006) 677–684.
[26] J. Saunier, N. Chaix, F. Alloin, J.P. Belieres, J.Y. Sanchez, Electrochim. Acta 47 (2002) 1321–1326.
[27] D. Golodnitsky, G. Ardel, E. Peled, Solid State Ion. 85 (1996) 231–238.
[28] A.M. Elmer, P. Jannasch, Solid State Ion. 177 (2006) 573–579.
[29] J.R. MacCallum, C.A. Vincent (Eds.), Polymer Electrolytes Reviews-1, Elsevier, London, 1987.
[30] H. Nithya, S. Selvasekarapandian, P. Christopher Selvin, D. Arun Kumar, J. Kawamura, Electrochim. Acta 66 (2012) 110–120.
[31] H.S. Kim, J.H. Shin, S.I. Moona, S.P. Kim, Electrochim. Acta 48 (2003) 1573–1578.
[32] J. Choa, B. Park, J. Power Sources 92 (2001) 35–39.
[33] K. Nishikawa, Y. Fukunaka, T. Sakka, Y.H. Ogata, J.R. Selman, Electrochim. Acta 53 (2007) 218–223.
[34] S.S. Zhang, K. Xu, T.R. Jow, J. Power Sources 113 (2003) 166–172.